PERGAMON

Mechatronics 14 (2004) 69–90

MECHATRONICS

Command shaping techniques for vibration control of a flexible robot manipulator

Z. Mohamed, M.O. Tokhi *

Department of Automatic Control and Systems Engineering, The University of Sheffield, Mappin Street, Sheffield S1 3JD, UK

Accepted 27 January 2003

Abstract

This paper presents an investigation into development of feed-forward control strategies for vibration control of a flexible robot manipulator using command shaping techniques based on input shaping, low-pass and band-stop filtering. A constrained planar single-link flexible manipulator is considered and the dynamic model of the system is derived using the finite element method. An unshaped bang–bang torque input is used to determine the characteristic parameters of the system for design and evaluation of the control techniques. Feed-forward controllers are designed based on the natural frequencies and damping ratios of the system. Simulation results of the response of the manipulator to the shaped and filtered inputs are presented in time and frequency domains. Performances of the techniques are assessed in terms of level of vibration reduction at resonance modes, speed of response, robustness and computational complexity. The effects of number of impulse sequence and filter order on the performance of the system are investigated. Finally, a comparative assessment of the input shaping and input-filtering techniques is presented and discussed.

1. Introduction

Most existing robotic manipulators are designed and built in a manner to maximise stiffness, in an attempt to minimise system vibration and achieve good positional accuracy. High stiffness is achieved by using heavy material. As a consequence, such robots are usually heavy with respect to the operating payload. This,

* Corresponding author. Tel.: +44-114-222-5617; fax: +44-114-222-5661.
E-mail address: o.tokhi@sheffield.ac.uk (M.O. Tokhi).

0957-4158/$ - see front matter © 2003 Elsevier Ltd. All rights reserved.
doi:10.1016/S0957-4158(03)00013-8

in turn, limits the speed of operation of the robot manipulation, increases the size of actuator, boosts energy consumption and increases the overall cost. Moreover, the payload to robot weight ratio, under such situations, is low. In order to solve these problems, robotic systems are designed to be lightweight and thus possess some level of flexibility. Conversely, flexible robot manipulators exhibit many advantages over their rigid counterparts: they require less material, are lighter in weight, have higher manipulation speed, lower power consumption, require smaller actuators, are more maneuverable and transportable, are safer to operate due to reduced inertia, have enhanced back-drive ability due to elimination of gearing, have less overall cost and higher payload to robot weight ratio [1].

However, the control of flexible robot manipulators to maintain accurate positioning is an extremely challenging problem. Due to the flexible nature and distributed characteristics of the system, the dynamics are highly non-linear and complex. Problems arise due to precise positioning requirement, vibration due to system flexibility, the difficulty in obtaining accurate model of the system and non-minimum phase characteristics of the system [2,3]. Therefore, flexible manipulators have not been favoured in production industries, due to un-attained end-point positional accuracy requirements in response to input commands. In this respect, a control mechanism that accounts for both the rigid body and flexural motions of the system is required. If the advantages associated with lightness are not to be sacrificed, accurate models and efficient control strategies for flexible robot manipulators have to be developed.

The control strategies for flexible robot manipulator systems can be classified as feed-forward (open-loop) and feedback (closed-loop) control schemes. Feed-forward techniques for vibration suppression involve developing the control input through consideration of the physical and vibrational properties of the system, so that system vibrations at response modes are reduced. This method does not require any additional sensors or actuators and does not account for changes in the system once the input is developed. On the other hand, feedback-control techniques use measurement and estimations of the system states to reduce vibration. Feedback controllers can be designed to be robust to parameter uncertainty. For flexible manipulators, feed-forward and feedback control techniques are used for vibration suppression and end-point position control respectively. An acceptable system performance without vibration that accounts for system changes can be achieved by developing a hybrid controller consisting of both control techniques. Thus, a properly designed feed-forward controller is required. Furthermore, the complexity of the required feedback controllers can be reduced.

A number of techniques have been proposed as feed-forward control strategies for flexible manipulators. Aspinwall [4] has used Fourier expansion for the forcing function through which the controller parameters are chosen so as to reduce the peaks of the frequency spectrum at discrete points. This only eliminates a few of the peaks and leaves some modes excited. Swigert [5] has derived an approximately shaped torque that minimises residual vibration and the effect of parameter variations that affect the modal frequencies. However, the forcing function is not time optimal. Several researchers have presented and studied the application of computed

torque techniques for control of flexible manipulators [6,7]. In this approach, the system is first modelled in detail. By inverting the desired output trajectory, the required input needed to generate that trajectory is computed. For linear systems, this might involve dividing the frequency spectrum of the trajectory by the transfer function of the system, thus obtaining the frequency spectrum of the input. For nonlinear systems, this technique involves inverting the equations describing the model. However, this technique suffers from several problems [8]. These are due to inaccuracy of a model, selection of poor trajectory to guarantee that the system can follow it, sensitivity to variations in system parameters and response time penalties for a causal input.

Bang–bang control involves the utilisation of single and multiple-switch bang–bang control functions [9]. Bang–bang control functions require accurate selection of switching time, depending on the representative dynamic model of the system. Minor modelling errors could cause switching error, and thus, result in a substantial increase in the residual vibrations. Although, utilisation of minimum energy inputs has been shown to eliminate the problem of switching times that arise in the bang–bang input, the total response time becomes longer [9,10]. Meckl and Seering [11,12] have examined the construction of input functions from either ramped sinusoids or versine (1 – cosine) functions. This approach involves adding up harmonics of one of these template functions. If all harmonics were included, the input would be a time optimal rectangular input function. The harmonics that have significant spectral energy at the natural frequencies of the system are eliminated. The resulting input which is given to the system approaches the rectangular shape, but does not significantly excite the resonances. The method has subsequently been tested on a cartesian robot, achieving considerable reduction in the residual vibrations [10].

Another promising technique for feed-forward control of a flexible robot manipulator is the command shaping technique. A significant amount of work on shaped command input based on filtering techniques has been reported. In this approach, a shaped torque input is developed on the basis of extracting the input energy around the natural frequencies of the system, so that the vibration of the flexible robot manipulator during and after the movement is reduced. Various filtering techniques have been employed. These include low-pass filters, band-stop filters and notch filters [13–16]. It has been shown that better performance in the reduction of level of vibration of the system is achieved using low-pass filters.

An approach in command-shaping techniques known as input shaping has been proposed by Singer and co-workers which is currently receiving considerable attention in vibration control [8,17]. Since its introduction, the method has been investigated and extended. The method involves convolving a desired command with a sequence of impulses known as input shaper. The shaped command that results from the convolution is then used to drive the system. Design objectives are to determine the amplitude and time locations of the impulses, so that the shaped command reduces the detrimental effects of system flexibility. These parameters are obtained from the natural frequencies and damping ratios of the system. Using this method, a response without vibration can be achieved, however, with a slight time delay

approximately equal to the length of the impulse sequence. The method has been shown to be the most effective in reducing vibration in flexible plants [18]. The more impulses are used, the more robust the system becomes to flexible mode parameter changes but the longer the delay introduced into the system response. Previous investigations have shown that the input shaper can be designed to account for modelling errors in natural frequencies and damping ratio [19,20].

The aim of this investigation is to develop feed-forward control schemes for vibration control of a flexible robot manipulator system using input shaping and filtering techniques and to provide a comparative assessment of these techniques. In this work, low-pass and band-stop filters are considered. A constrained planar single-link flexible robot manipulator is considered and the dynamic model of the system is derived using the finite element (FE) method. Previous investigations have shown that the FE method gives an acceptable dynamic characterisation of the actual system. Moreover, a single element is sufficient to describe the dynamic behaviour of the manipulator reasonably well [21,22]. Initially, the system is excited with a single-switch bang–bang torque input and the system parameters are obtained. Then the input shapers and filters are designed based on the properties of the manipulator and used for pre-processing the input, so that no energy is put into the system at resonance modes. Performances of the developed controllers are assessed in terms of level of vibration reduction at resonance modes, speed of response, robustness to errors in vibration frequency and computational complexity. These are accomplished by comparing the system response to that with the unshaped bang–bang input. Moreover, the effects of number of impulses and filter order on the performance of the system are investigated. Simulation results in time and frequency domains of the response of the flexible manipulator to the unshaped, shaped and filtered inputs are presented. The robustness of the control schemes is assessed with up to 30% error tolerance in vibration frequencies. Finally, a comparative assessment of the performances of the feed-forward control strategies in vibration suppression of the manipulator is presented and discussed.

2. The flexible manipulator system

A description of the single-link flexible manipulator system considered in this work, is shown in Fig. 1, where **XOY** and **POQ** represent the stationary and moving co-ordinates frames respectively, τ represents the applied torque at the hub. E, I, ρ, A, I_h and M_p represent the Young modulus, area moment of inertia, mass density per unit volume, cross-sectional area, hub inertia and payload mass of the manipulator respectively. In this work, the motion of the manipulator is confined to the **XOY** plane. Since the manipulator is long and slender, transverse shear and rotary inertia effects are neglected. This allows the use of the Bernoulli–Euler beam theory to model the elastic behaviour of the manipulator. The manipulator is assumed to be stiff in vertical bending and torsion, allowing it to vibrate dominantly in the horizontal direction and thus, the gravity effects are neglected. Moreover, the manipu-

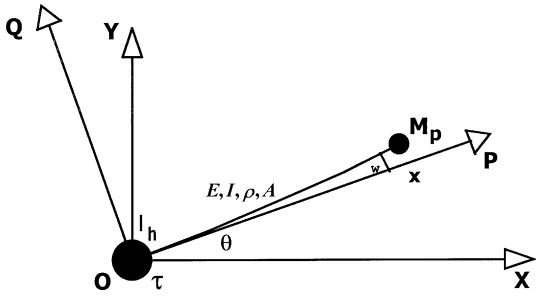

Fig. 1. Description of the flexible manipulator system.

lator is considered to have constant cross-section and uniform material properties throughout. In this study, an aluminium type flexible manipulator of dimensions $900 \times 19.008 \times 3.2004$ mm^3, $E = 71 \times 10^9$ N/m^2, $I = 5.1924$ m^4 and $\rho = 2710$ kg/m^3 is considered.

3. Modelling of the flexible manipulator

This section briefly describes modelling of the flexible robot manipulator system, as basis of a simulation environment for development of feed-forward control strategies for vibration control of the system. In this investigation, the FE method with 10 elements is considered in characterising the dynamic behaviour of the manipulator incorporating structural damping and hub inertia. The equations of motion are expressed in a state-space form. Simulation results of the dynamic behaviour of the manipulator are presented in the time and frequency domains.

The main steps in an FE analysis include (1) discretisation of the structure into elements; (2) selection of an approximating function to interpolate the result; (3) derivation of the basic element equation; (4) calculation of the system equation; (5) incorporation of the boundary conditions and (6) solving the system equation with the inclusion of the boundary conditions. In this manner, the flexible manipulator is treated as an assemblage of n elements and the development of the algorithm can be divided into three main parts: the FE analysis, state-space representation and obtaining and analysing the system response.

For a small angular displacement $\theta(t)$ and a small elastic deflection $w(x,t)$, the total displacement $y(x,t)$ of a point along the manipulator at a distance x from the hub can be described as a function of both the rigid body motion $\theta(t)$ and elastic deflection $w(x,t)$ measured from the line OX as

$$y(x,t) = x\theta(t) + w(x,t)$$

Using the FE method and kinetic and potential energies of an element, yields the element mass matrix, M_n and stiffness matrix, K_n as [22]

$$M_n = \frac{\rho A l}{420}\begin{bmatrix} m_{11} & m_{12} & m_{13} & m_{14} & m_{15} \\ m_{21} & 156 & 22l & 54 & -13l \\ m_{31} & 22l & 4l^2 & 13l & -3l^2 \\ m_{41} & 54 & 13l & 156 & -22l \\ m_{51} & -13l & -3l^2 & -22l & 4l^2 \end{bmatrix}$$

$$K_n = \frac{EI}{l^3}\begin{bmatrix} 0 & 0 & 0 & 0 & 0 \\ 0 & 12 & 6l & -12 & 6l \\ 0 & 6l & 4l^2 & -6l & 2l^2 \\ 0 & -12 & -6l & 12 & -6l \\ 0 & 6l & 2l^2 & -6l & 4l^2 \end{bmatrix}$$

where

$$\begin{aligned} m_{11} &= 140l^2(3n^2 - 3n + 1) \\ m_{12} &= m_{21} = 21l(10n - 7) \\ m_{13} &= m_{31} = 7l^2(5n - 3) \\ m_{14} &= m_{41} = 21l(10n - 3) \\ m_{15} &= m_{51} = -7l^2(5n - 2) \end{aligned}$$

l is the elemental length of the manipulator and n is number of elements.

Assembling the element mass and stiffness matrices and utilising the Lagrange equation of motion, the desired dynamic equations of motion of the system can be obtained as

$$M\ddot{Q}(t) + D\dot{Q}(t) + KQ(t) = F(t) \tag{1}$$

where M, D and K are global mass, damping and stiffness matrices of the manipulator respectively. The damping matrix is obtained by assuming that the manipulator exhibits the characteristic of Rayleigh damping. $F(t)$ is a vector of external forces. $Q(t)$ is a nodal displacement vector given as

$$Q(t) = [\theta \quad w_0 \quad \theta_0 \quad \cdots \quad w_n \quad \theta_n]^{\mathrm{T}}$$

where $w_n(t)$ and $\theta_n(t)$ are the flexural and angular deflections at the end point of the manipulator respectively.

With 10 elements, the M, D and K matrices in Eq. (1) are of size $m \times m$ and $F(t)$ is of size $m \times 1$, where $m = 21$. For the manipulator, considered as a pinned-free arm with the applied torque τ at the hub, the flexural and angular deflections, velocity and acceleration are all zero at the hub at $t = 0$ and the external force is $F(t) = [\tau \ 0 \ \cdots \ 0]^{\mathrm{T}}$. Moreover, in this work, it is assumed that $Q(0) = 0$.

The matrix differential equation in Eq. (1) can be represented in a state-space form as

$$\begin{aligned} \dot{v} &= Av + Bu \\ y &= Cv \end{aligned}$$

where

$$\mathbf{A} = \left[\begin{array}{c|c} 0_m & I_m \\ \hline -M^{-1}K & -M^{-1}D \end{array}\right], \quad \mathbf{B} = \left[\begin{array}{c} 0_{m\times 1} \\ \hline M^{-1} \end{array}\right]$$

$$\mathbf{C} = [I_{2m}]$$

0_m is an $m \times m$ null matrix, I_m is an $m \times m$ identity matrix, $0_{m\times 1}$ is an $m \times 1$ null vector, $u = [\tau\ 0\ \cdots\ 0]^{\mathrm{T}}$, $v = [\theta\ w_1\ \theta_1\ \cdots\ w_n\ \theta_n\ \dot{\theta}\ \dot{w}_1\ \dot{\theta}_1\ \ldots\ \dot{w}_n\ \dot{\theta}_n]^{\mathrm{T}}$. Solving the state-space matrices gives the vector of states v, that is, the angular, nodal flexural and angular displacements and velocities. Further details of the derivation of the dynamic equations of motion of the flexible manipulator using the FE method are given in [22].

To assess the adequacy of the FE model, simulation results of the dynamic behaviour of the flexible manipulator using 10 elements are presented in the time and frequency domains. Previous experimental study on the actual flexible manipulator has shown that the damping ratio of the system ranges from 0.024 to 0.1 [23]. In this work, the damping ratios of the system were deduced as 0.026, 0.038 and 0.04 for the first, second and third modes respectively. Fig. 2a shows a single-switch bang–bang signal of amplitude 0.3 N m used as an input torque, applied at the hub of the manipulator. Fig. 2b shows the corresponding spectral density (SD). A bang–bang torque has a positive (acceleration) and negative (deceleration) period allowing the manipulator to, initially, accelerate and then decelerate and eventually stop at a target location. Three system responses namely hub-angle, hub-velocity and end-point residual with SD of the end-point residual are obtained. The results are recorded with a sampling frequency of 500 Hz. In this work, the first three modes of vibration are considered, as these dominantly characterise the behaviour of the flexible manipulator.

Fig. 3 shows the response of the flexible manipulator system with the SD of the end-point residual using 10 elements. These results were considered as the system

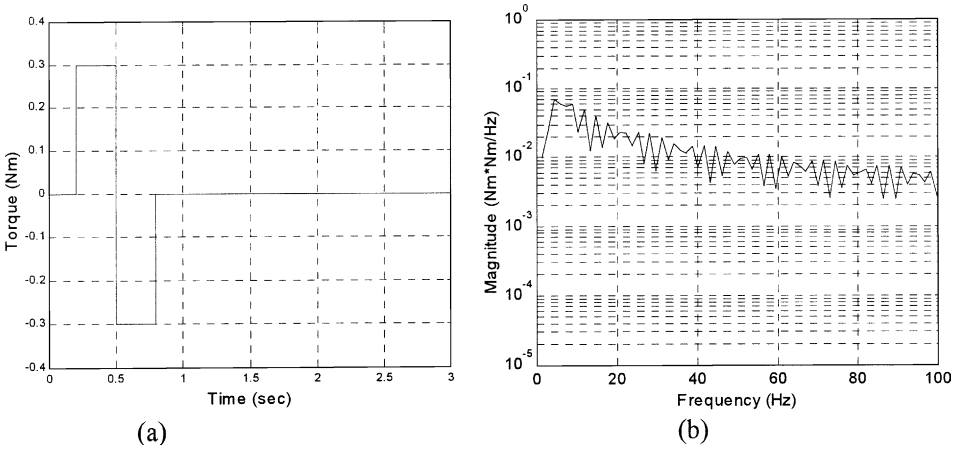

Fig. 2. The bang–bang torque input. (a) Time domain, (b) SD.

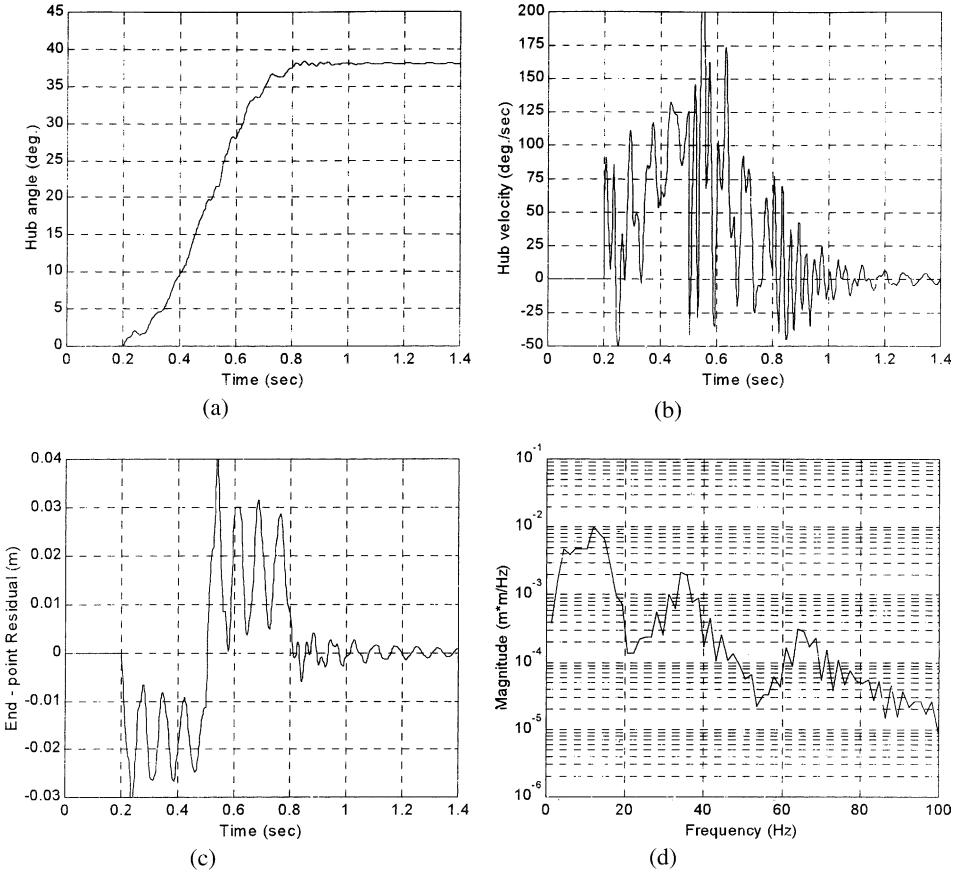

Fig. 3. Response of the flexible manipulator to the bang–bang torque input. (a) Hub angle, (b) hub velocity, (c) end-point residual, (d) SD of end-point residual.

response to the unshaped input and subsequently will be used to evaluate the performance of the command shaping techniques. It is noted that a steady-state hub-angle level of 38° was achieved within rise time of 0.386 s and settling time of 0.788 s. The rise and settling times were calculated on the basis of response duration of 10–90% and ±2% of the steady-state value respectively. Note that vibrations occur during movement of the manipulator, as evidenced in the hub-velocity and end-point residual responses. The end-point residual response was found to oscillate between 0 and 30 mm. The residual motion of the system is found to be characterised by the first three modes of vibration. Resonance frequencies of the system were obtained by transforming the time-domain representation of the end-point residual of the system into frequency-domain using FFT analysis. As demonstrated in Fig. 3, the vibration frequencies of the system were obtained as 12, 35 and 65 Hz. The magnitudes of SD of the end-point residual response were obtained as 0.01, 0.002 and 0.0003 m^2/Hz for

the first three resonance modes respectively. Previous experimental study of the actual flexible manipulator has resulted vibration frequencies of 11.72, 35.15 and 65.6 Hz with a steady-state hub-angle response of 38° [22]. These are reasonably close to those obtained from the response of the system using 10 elements. Thus the model provides sufficient accuracy for development and evaluation of control techniques.

4. Feed-forward control techniques

In this section, input shaping, low-pass and band-stop filtering techniques are introduced for vibration control of a flexible robot manipulator.

4.1. Input shaping

As described in Section 1, the input shaping method involves convolving a desired command with a sequence of impulses. The design objectives are to determine the amplitude and time location of the impulses. The method is briefly described in this section [8]. A vibratory system of any order can be modelled as a superposition of second order systems each with a transfer function

$$G(s) = \frac{\omega^2}{s^2 + 2\xi\omega s + \omega^2}$$

where ω is the natural frequency and ξ is the damping ratio of the system. Thus, the impulse response of the system can be obtained as

$$y(t) = \frac{A\omega}{\sqrt{1-\xi^2}} e^{-\xi\omega(t-t_0)} \sin\left(\omega\sqrt{1-\xi^2}(t-t_0)\right)$$

where A and t_0 are the strength and time of the impulse respectively. Further, the response to a sequence of impulses can be obtained by superposition of the impulse responses. Thus, for N impulses, with $\omega_d = \omega(\sqrt{1-\xi^2})$, the impulse response can be expressed as

$$y(t) = M\sin(\omega_d t + \beta)$$

where

$$M = \sqrt{\left(\sum_{i=1}^{N} B_i \cos\phi_i\right)^2 + \left(\sum_{i=1}^{N} B_i \sin\phi_i\right)^2},$$

$$B_i = \frac{A_i\omega}{\sqrt{1-\xi^2}} e^{-\xi\omega(t-t_0)} \quad \text{and} \quad \phi_i = \omega_d t_i$$

A_i and t_i are the strengths and times of the impulses.

The residual single mode vibration amplitude of the impulse response is obtained at the time of the last impulse, t_N as

$$V = \sqrt{V_1^2 + V_2^2} \tag{2}$$

where

$$V_1 = \sum_{i=1}^{N} \frac{A_i \omega_n}{\sqrt{1-\zeta^2}} e^{-\zeta\omega_n(t_N - t_i)} \cos(\omega_d t_i), \quad V_2 = \sum_{i=1}^{N} \frac{A_i \omega_n}{\sqrt{1-\zeta^2}} e^{-\zeta\omega_n(t_N - t_i)} \sin(\omega_d t_i)$$

To achieve zero vibration after the last impulse, it is required that both V_1 and V_2 in Eq. (2) are independently zero. Furthermore, to ensure that the shaped command input produces the same rigid body motion as the unshaped command, it is required that the sum of strengths of the impulses is unity. To avoid response delay, the first impulse is selected at time $t_1 = 0$. Hence by setting V_1 and V_2 in Eq. (2) to zero, $\sum_{i=1}^{N} A_i = 1$ and solving yields a two-impulse sequence with parameters as

$$\begin{aligned} &t_1 = 0, \quad t_2 = \frac{\pi}{\omega_d} \\ &A_1 = \frac{1}{1+K}, \quad A_2 = \frac{K}{1+K} \end{aligned} \tag{3}$$

where

$$K = e^{-\frac{\xi\pi}{\sqrt{1-\xi^2}}}$$

The robustness of the input shaper to error in natural frequencies of the system can be increased by setting $dV/d\omega = 0$, where $dV/d\omega$ is the rate of change of V with respect to ω.

Setting the derivative to zero is equivalent of producing small changes in vibration with corresponding changes in the natural frequency. Thus, additional constraints are incorporated into the equation, which after solving yields a three-impulse sequence with parameters as

$$\begin{aligned} &t_1 = 0, \quad t_2 = \frac{\pi}{\omega_d}, \quad t_3 = 2t_2 \\ &A_1 = \frac{1}{1+2K+K^2}, \quad A_2 = \frac{2K}{1+2K+K^2}, \quad A_3 = \frac{K^2}{1+2K+K^2} \end{aligned} \tag{4}$$

where K is as in Eq. (3). The robustness of the input shaper can further be increased by taking and solving the second derivative of the vibration in Eq. (2). Similarly, this yields a four-impulse sequence with parameters as

$$\begin{aligned} &t_1 = 0, \quad t_2 = \frac{\pi}{\omega_d}, \quad t_3 = 2t_2, \quad t_4 = 3t_2 \\ &A_1 = \frac{1}{1+3K+3K^2+K^3}, \quad A_2 = \frac{3K}{1+3K+3K^2+K^3}, \\ &A_3 = \frac{3K^2}{1+3K+3K^2+K^3}, \quad A_4 = \frac{K^3}{1+3K+3K^2+K^3} \end{aligned} \tag{5}$$

where K is as in Eq. (3).

To handle higher vibration modes, an impulse sequence for each vibration mode can be designed independently. Then the impulse sequences can be convoluted together to form a sequence of impulses that attenuates vibration at higher modes. For any vibratory system, the vibration reduction can be accomplished by convolving any desired system input with the impulse sequence. This yields a shaped input that drives the system to a desired location without vibration.

4.2. Filtering techniques

Command shaping based on filtering techniques is developed on the basis of extracting the energies around the vibration frequencies using filtering techniques. The filters are thus used for pre-processing the input signal so that no energy is put into the system at frequencies corresponding to the resonance modes of the system. In this manner, the resonance modes of the system are not excited, leading to a vibration-free motion of the system. This can be realised by employing either low-pass or band-stop filters. In the former, the filter is designed with a cut-off frequency lower than the first resonance mode of the system. In the latter case, band-stop filters with centre frequencies at the resonance modes of the system are designed. This will require one filter for each flexible mode of the system. The band-stop filters thus designed are then implemented in cascade to pre-process the input signal. There are various filter types such as Butterworth, Chebyshev and Elliptic that can be designed and employed [24]. In this investigation, infinite impulse response (IIR) Butterworth low-pass and band-stop filters are examined.

5. Implementation and results

The feed-forward control techniques were designed on the basis of vibration frequencies and damping ratios of the flexible manipulator system. These were obtained from the developed flexible manipulator environment using 10 elements, as presented in the previous section. As demonstrated, the natural frequencies of the system were obtained as 12, 35 and 65 Hz and the damping ratios were deduced as 0.026, 0.038 and 0.04 for the first three modes of vibration respectively. For evaluation of robustness, the control techniques were designed based on 30% error tolerance in the natural frequencies. As a consequence, the system vibration modes were considered as 15.6, 45.5 and 84.5 Hz under this situation. The input shapers and filters thus designed were used for pre-processing the bang–bang torque input. The shaped and filtered torque inputs were then applied to the system in an open-loop configuration as shown in Fig. 4 to reduce the vibrations of the manipulator. In this process, the shaped and filtered inputs were designed within the Matlab environment with a sampling frequency of 500 Hz and implemented on a Pentium III 650 MHz processor.

Simulation results of the response of the flexible manipulator to the shaped and filtered inputs are presented in this section in the time and frequency domains. To verify the performance of the control techniques, the results are examined in

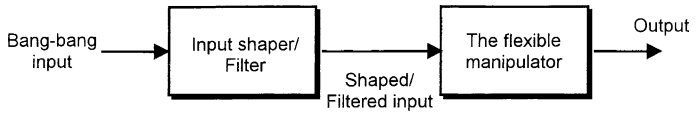

Fig. 4. Block diagram of the feed-forward control configuration.

comparison to the unshaped bang–bang torque input for a similar input level in each case. Similarly, three system responses are investigated namely the hub-angle, hub-velocity and end-point residual. Four criteria are used to evaluate the performances of the control schemes:

(1) Level of vibration reduction at resonance modes. This is accomplished by comparing the shaped input response with the response to the unshaped input. The results are presented in dB.
(2) The time response specifications. Parameters that are evaluated are settling time, rise time and the magnitude of vibration.
(3) Robustness to parameter uncertainty. To examine the robustness of the techniques, the system performance is assessed with 30% error tolerance in natural frequencies.
(4) Computational complexity. Execution times to develop the shaped and filtered inputs are calculated. This is an important aspect in real-time implementation of the controller.

5.1. Input shaping

Using the parameters of the system, input shapers with two- and four-impulse sequences for the first three modes of vibration were designed. The strengths and time locations of the impulses were obtained by solving Eqs. (3) and (5) respectively. Similarly, input shapers with error in natural frequencies were also evaluated. With exact natural frequency, locations of the second impulse were obtained at 0.0385, 0.0143 and 0.0077 s for the three resonance modes respectively. On the other hand, with error in natural frequencies, locations of the second impulse were obtained at 0.0296, 0.0110 and 0.0059 s. Strengths of the input shapers were accordingly obtained and used with both the exact and erroneous natural frequencies. For digital implementation of the input shapers, locations of the impulses were selected at the nearest sampling time. Fig. 5 shows the shaped inputs and the corresponding SDs using input shaping. It is noted that with higher number of impulses, the magnitudes of the SD at resonance modes reduce. Moreover, the range of frequency covered around the resonance modes increases.

Fig. 6 shows the responses of the flexible manipulator with the SD of the end-point residual to the shaped input using two- and four-impulse sequences. It is noted that the magnitudes of vibration at the resonance modes of the system, with the hub-angle, hub-velocity and end-point residual responses, have significantly been re-

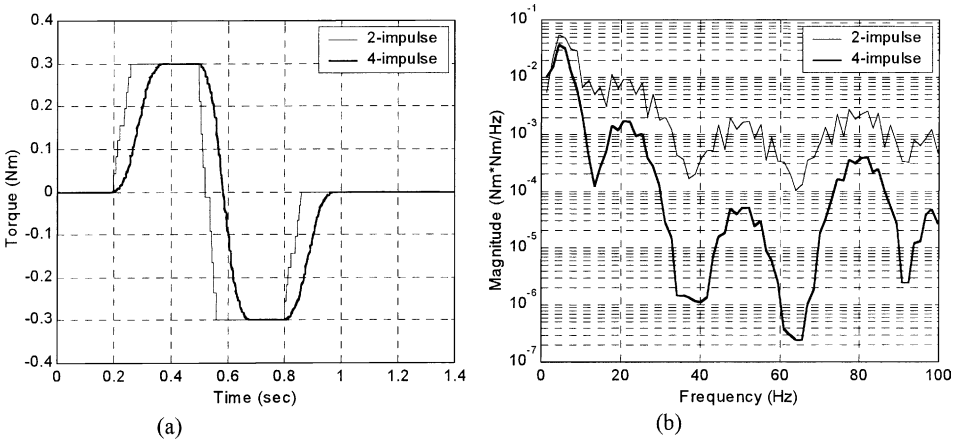

Fig. 5. Shaped torque inputs using two- and four-impulse sequences. (a) Time domain, (b) SD.

duced. These can be observed by comparing the system responses to the unshaped input (Fig. 3). The oscillations in the end-point residual response were found to have almost reduced to zero. Lower magnitudes of the SDs as compared to the unshaped input were achieved. The rise times of the hub-angle response were obtained as 0.370 and 0.387 s and the settling times as 0.820 and 0.878 s with the two- and four-impulse sequences respectively. These results show that the hub-angle response is slower than the response to the unshaped input. It is noted that the level of vibration reduction increases with higher number of impulses, at the expense of increase in the delay in the response of the system.

Fig. 7 shows the response of the manipulator to the shaped input using two- and four-impulse sequences with 30% error in natural frequencies. This is used to examine the robustness of the technique. As noted, the level of reduction in the vibration of the manipulator is slightly less than the case without error. However, it is noted that significant vibration reduction was achieved, especially with a four-impulse sequence.

5.2. Filtered inputs

Using the low-pass filter, the input energy at all frequencies above the cut-off frequency can be attenuated. In this study, low-pass filters with cut-off frequency at 75% of the first vibration mode were designed. Thus, for the flexible manipulator, the cut-off frequencies of the filters were selected as 9 and 11.7 Hz for the two cases of exact and 30% erroneous natural frequencies respectively. On the other hand, using the band-stop filter, the input energy at selected (dominant) resonance modes of the system can be attenuated. In this study, band-stop filters with bandwidth of 10 Hz were designed for the first three resonance modes. Similarly, the filters were designed

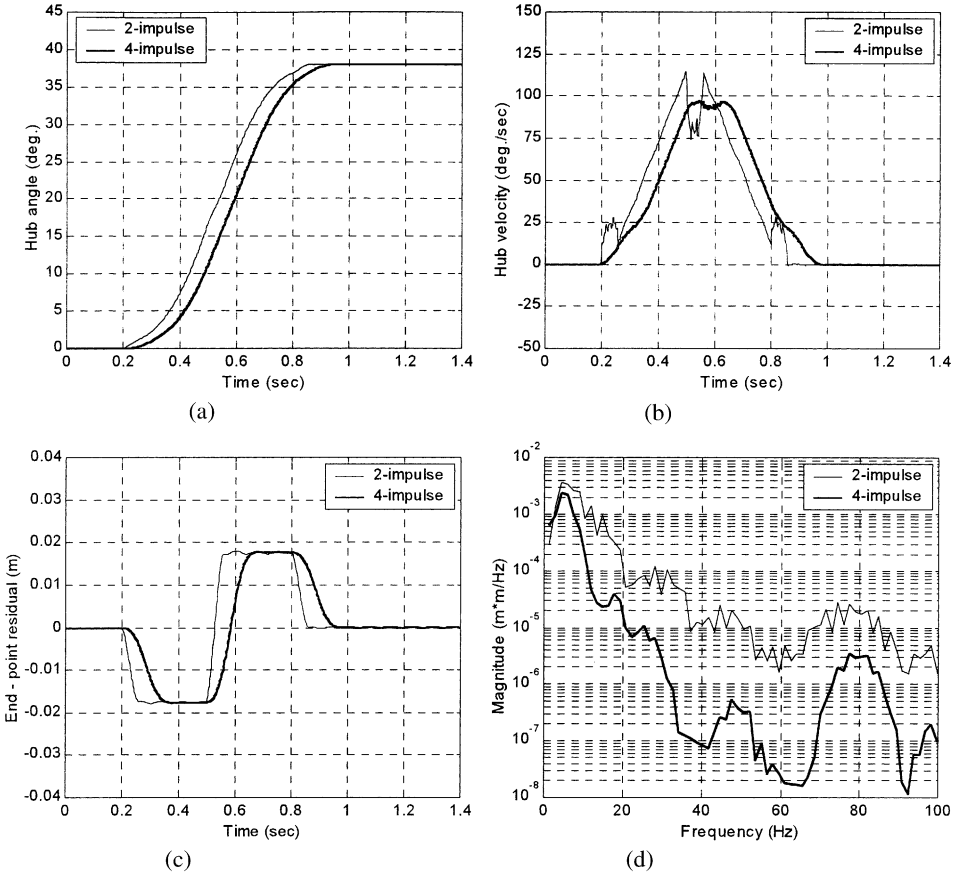

Fig. 6. Response of the flexible manipulator to the shaped inputs with exact natural frequencies. (a) Hub angle, (b) hub velocity, (c) end-point residual, (d) SD of end-point residual.

with consideration of exact and 30% error in natural frequencies. Moreover, the filters were designed in each case with third and sixth orders. Thus, the effects of various orders of filtered inputs on the performance of the manipulator were also studied. The filtered torque inputs and the corresponding SDs with the low-pass and band-stop filters are shown in Figs. 8 and 9 respectively. It is noted that the magnitudes of the SDs at resonance modes reduced with higher filter orders.

Fig. 10 shows the responses of the flexible manipulator with the SD of the end-point residual to the filtered torque using third and sixth order Butterworth low-pass filters. It is noted from the responses that the system vibrations at resonance modes have been considerably reduced in comparison to the bang–bang torque input. In this case, a lower magnitude of the SD of the end-point residual was achieved. As expected, the level of reduction increases with higher filter orders. Using this control technique, the rise times of the hub-angle response were obtained as 0.368 and 0.374 s

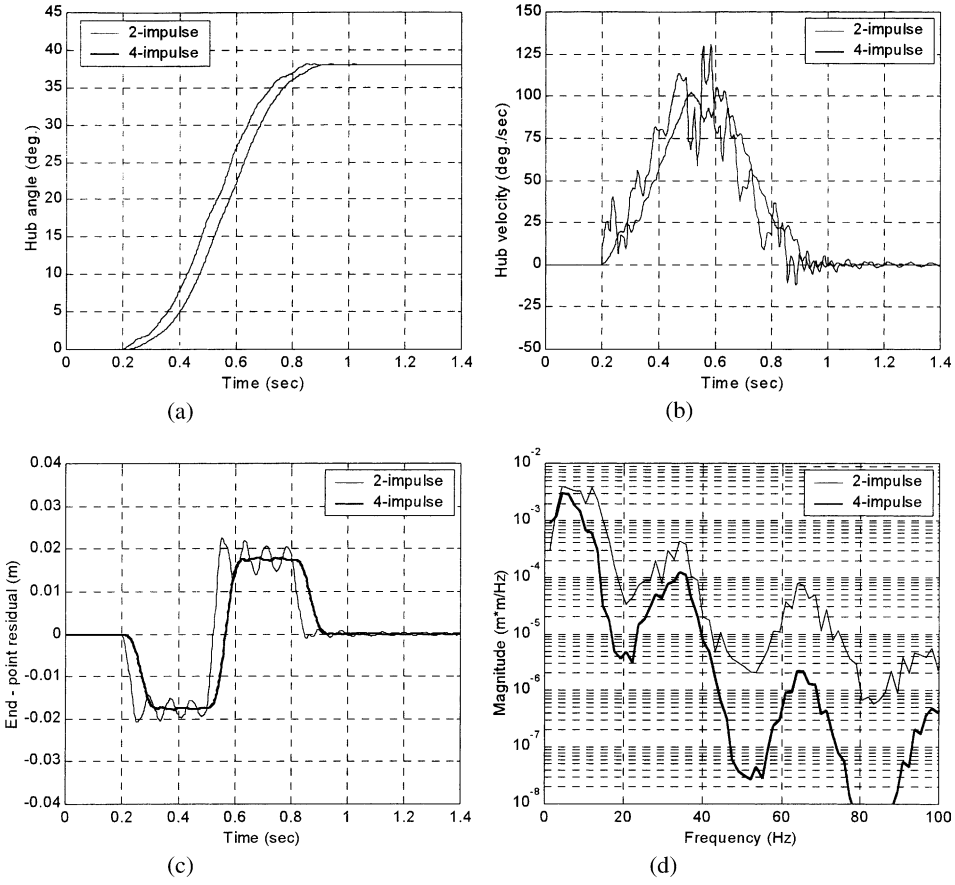

Fig. 7. Response of the flexible manipulator to the shaped inputs with 30% error in natural frequencies. (a) Hub angle, (b) hub velocity, (c) end-point residual, (d) SD of end-point residual.

and the settling times as 0.826 and 0.858 s with third and sixth order filters respectively. The robustness of the technique is demonstrated in Fig. 11, where the system response to the filtered torque with erroneous natural frequencies is shown. It is noted that relatively small reduction in the system vibration was achieved. This is evidenced in the magnitude of the time response and SDs.

The flexible manipulator response with the SD of the end-point residual to the third and sixth order Butterworth band-stop filtered inputs is shown in Fig. 12. It is noted that considerable amount of vibration reduction at the first three vibration modes was achieved in comparison with the response to the unshaped input. It is noted that the level of reduction increases with the filter order. The rise times of the hub-angle response were obtained as 0.368 and 0.370 s and the settling times as 0.812 and 0.830 s with third and sixth order filters respectively. Fig. 13 shows the response of the system to the filtered input with 30% error in vibration frequencies. It is noted

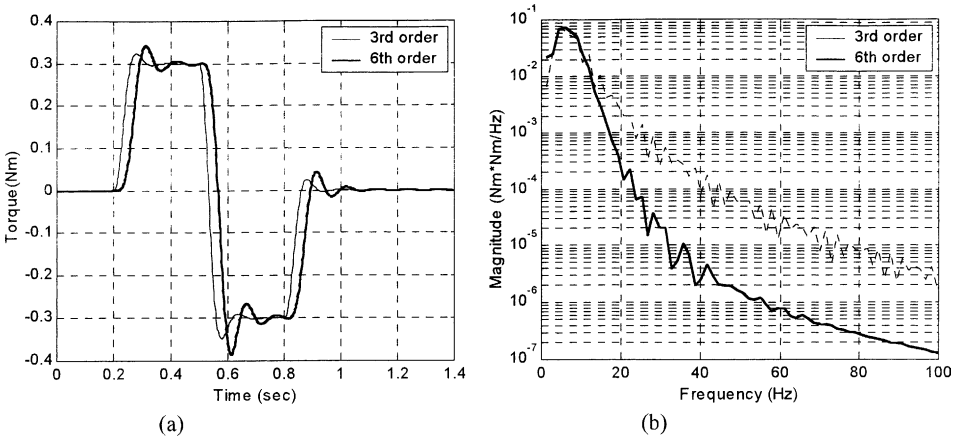

Fig. 8. Filtered torque inputs using the Butterworth low-pass filters. (a) Time domain, (b) SD.

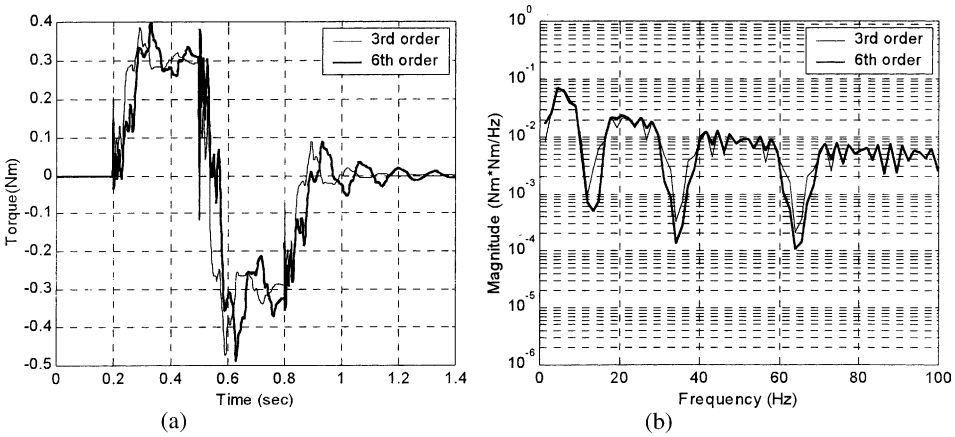

Fig. 9. Filtered torque inputs using the Butterworth band-stop filters. (a) Time domain, (b) SD.

that the level of vibration of the system at resonance modes was not significantly affected as compared to the unshaped input case. Moreover, no reduction was achieved at the second and third vibration modes. It is also noted that not much improvement was achieved with a higher filter order.

5.3. Comparative performance assessment

The level of vibration reduction achieved using the techniques with the end-point residual at the resonance modes in comparison to the bang–bang torque input is shown in Fig. 14. The result reveals that the highest performance in reduction of vibration of the flexible manipulator is achieved with the input shaping technique.

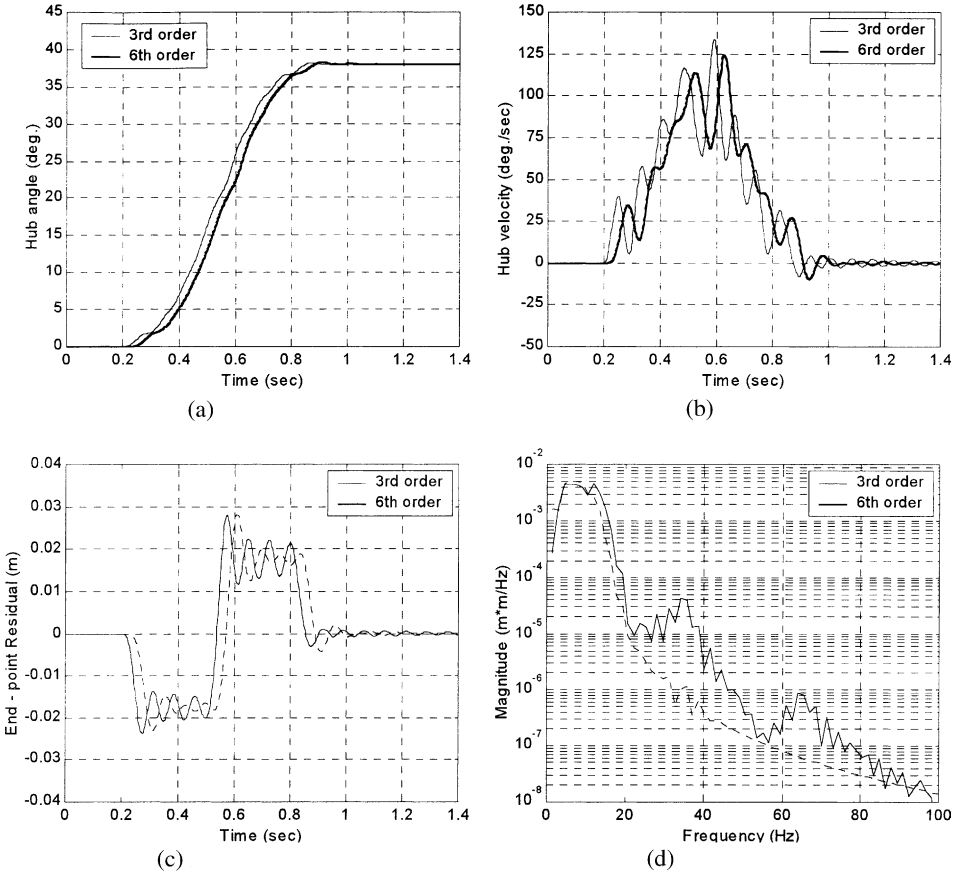

Fig. 10. Response of the flexible manipulator to the low-pass filtered inputs with exact natural frequencies. (a) Hub angle, (b) hub velocity, (c) end-point residual, (d) SD of end-point residual.

This is observed as compared to the low-pass and band-stop filtered inputs at the first three modes of vibration. The performance of the technique is also evidenced in the magnitude of vibration of the system in Figs. 6, 10 and 12. It is noted that better performance in vibration reduction of the system is achieved with the low-pass filtered input as compared to the band-stop filtered input. This is mainly due to the higher level of input energy reduction achieved with the low-pass filter, especially at the second and third vibration modes. However, the band-stop filtered input gives higher reduction at the first mode of vibration. As expected, system responses were slower with the shaped and filtered inputs as compared to the system response to the unshaped input. It is also noted that the delay in the system response increases with the number of impulses and filter order. Comparisons of specifications of hub-angle responses given in previous sections demonstrate that the band-stop filtered input results in the fastest system response. However, it is noted

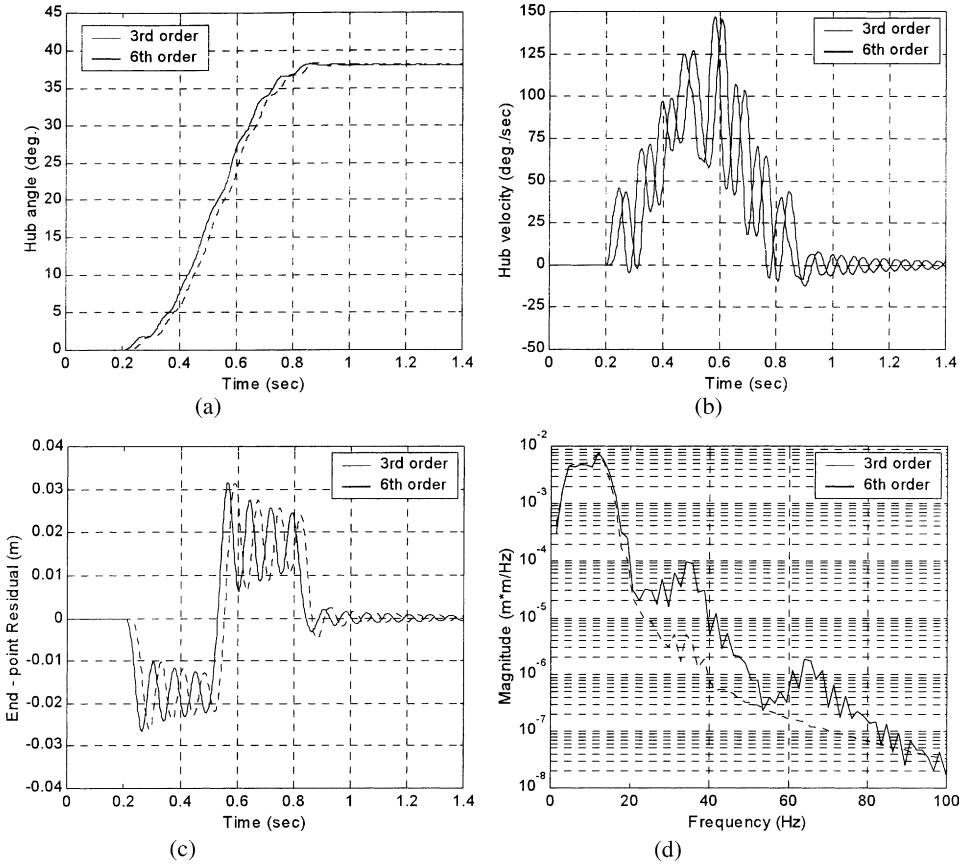

Fig. 11. Response of the flexible manipulator to the low-pass filtered inputs with 30% error in natural frequencies. (a) Hub angle, (b) hub velocity, (c) end-point residual, (d) SD of end-point residual.

that the differences in rise and settling times among the techniques are negligibly small.

The level of vibration reduction achieved using the techniques with erroneous natural frequencies is shown in Fig. 15. It is revealed that the highest robustness to parameter uncertainty is achieved with the input shaping technique. It is noted that the shaped input can successfully handle errors in the natural frequency especially with higher number of impulses. In this case, significant reduction in system vibration was achieved using a four-impulse sequence as compared to other control techniques. This is further revealed by comparing the magnitude of vibration of the system in Figs. 7, 11 and 13. The input shaping technique is more robust, as significant reduction was achieved at the first mode of vibration, which is the most dominant mode. The band-stop filtered input did not handle the error as only small amount of reduction of the system vibration was achieved, and there was no re-

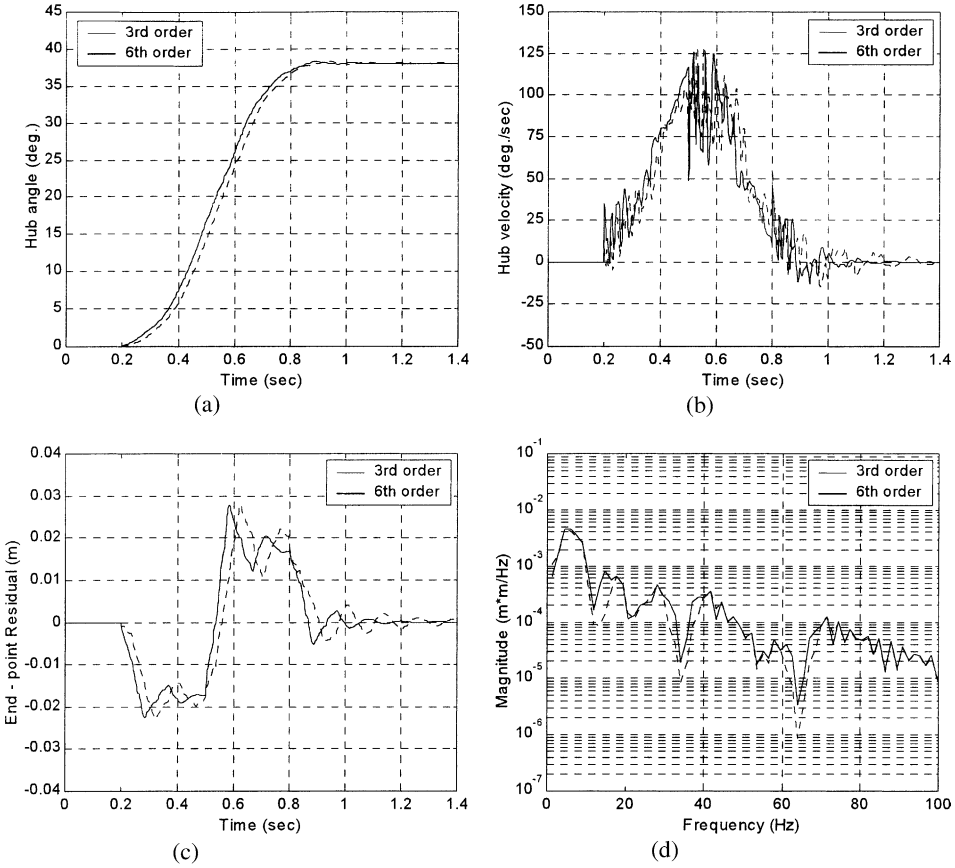

Fig. 12. Response of the flexible manipulator to the band-stop filtered inputs with exact natural frequencies. (a) Hub angle, (b) hub velocity, (c) end-point residual, (d) SD of end-point residual.

duction at the second and third modes of vibration. On the other hand, using the low-pass filter, a significant amount of attenuation of the system vibration was achieved at the second and third resonance modes. Moreover, the vibration reduction achieved with low-pass filtered inputs was higher than that with the shaped input at these resonance modes.

To study the computational complexity of the input shaping and filtering techniques, the execution times to develop the inputs were calculated. Within the Matlab environment, the execution times for input shaping, low-pass filter and the band-pass filter were obtained as 330, 110 and 130 ms respectively. This shows that development of the low-pass filtered input requires the lowest processing time. The longest processing time required for the input shaping technique is due to the convolution that has to be performed in this process. This information is vital to consider in designing and implementing such controllers in real time.

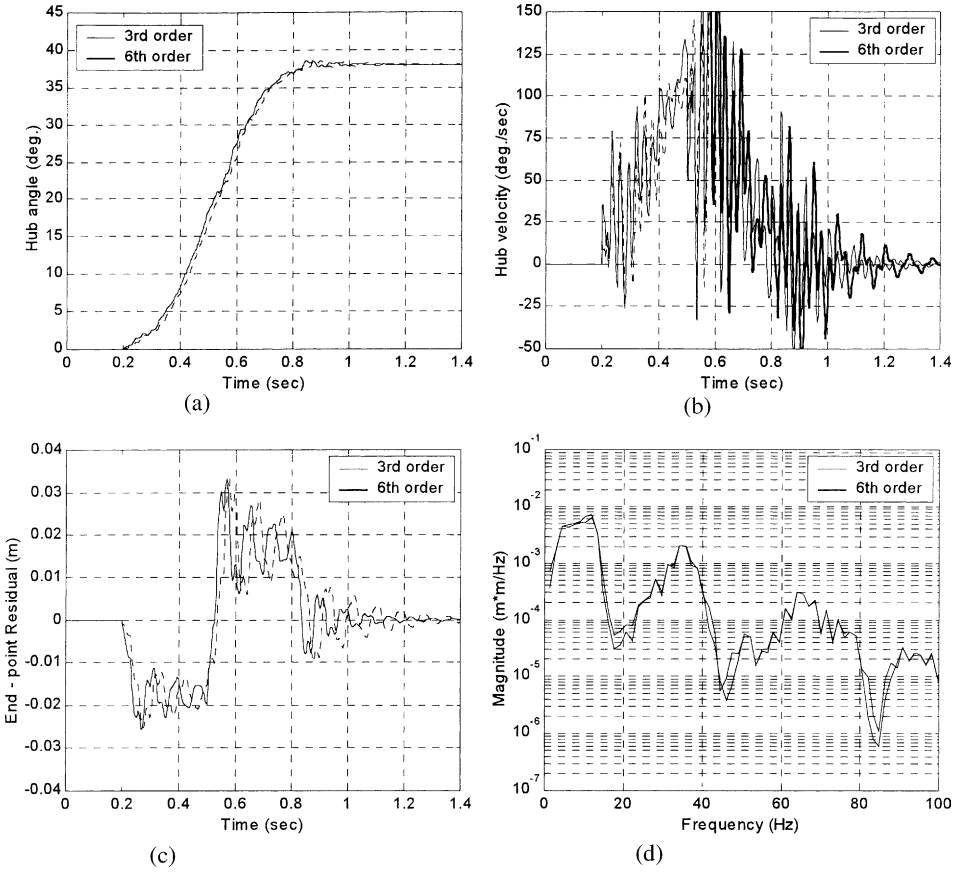

Fig. 13. Response of the flexible manipulator to the band-stop filtered inputs with 30% error in natural frequencies. (a) Hub angle, (b) hub velocity, (c) end-point residual, (d) SD of end-point residual.

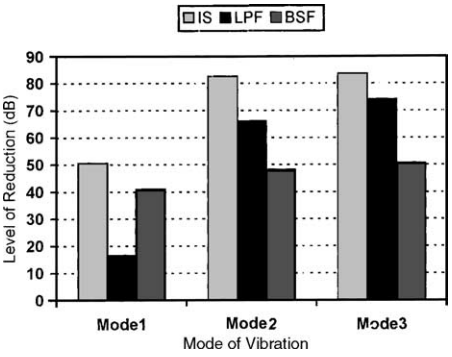

Fig. 14. Level of vibration reduction with the end-point residual response with exact natural frequencies using IS (four impulse), LPF (sixth order) and BSF (sixth order).

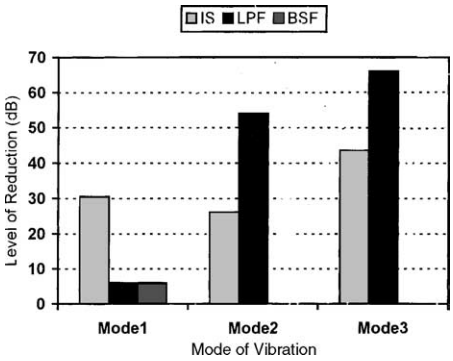

Fig. 15. Level of vibration reduction with the end-point residual response with 30% error in natural frequencies using IS (four impulse), LPF (sixth order) and BSF (sixth order).

6. Conclusion

The development of feed-forward control strategies for vibration control of a flexible robot manipulator using input shaping, low-pass and band-stop filtered input techniques has been presented. The dynamic model of the flexible manipulator utilising the FE method has been considered. The system response to the unshaped bang–bang torque input has been used to determine the parameters of the system for evaluation of the control strategies. Significant reduction in the system vibrations has been achieved with these control strategies. Performances of the techniques have been evaluated in terms of level of vibration reduction, speed of response, robustness and computational complexity. For the flexible manipulator and the specifications used in designing the input shapers and filters, the input shaping technique has been demonstrated to provide the best performance in vibration reduction, especially in terms of robustness to errors. The low-pass filtered input has been shown to perform better than the band-stop filtered input. However, the processing time in developing an input shaping command is longer as compared to that required for the filtered inputs.

References

[1] Book WJ, Majette M. Controller design for flexile distributed parameter mechanical arm via combined state-space and frequency domain techniques. Trans ASME: J Dyn Syst Meas Control 1983;105(4):245–54.
[2] Piedboeuf JC, Farooq M, Bayoumi MM, Labinaz G, Argoun MB. Modelling and control of flexible manipulators—revisited. Proceedings of 36th Midwest Symposium on Circuits and Systems, Detroit, 1983. p. 1480–3.
[3] Yurkovich S. Flexibility effects on performance and control. Robot Control 1992;(Part 8):321–3.
[4] Aspinwall DM. Acceleration profiles for minimising residual response. Trans ASME: J Dyn Syst Meas Control 1980;102(1):3–6.

[5] Swigert JC. Shaped torque techniques. J Guidance Control 1980;3(5):460–7.
[6] Bayo E. Computed torque for the position control of open-loop flexible robots. Proceedings of IEEE International Conference on Robotics and Automation, Philadelphia, 1988. p. 316–21.
[7] Moulin H, Bayo E. On the accuracy of end-point trajectory tracking for flexible arms by non-causal inverse dynamic solution. Trans ASME J Dyn Syst Meas Control 1991;113:320–4.
[8] Singer NC, Seering WP. Preshaping command inputs to reduce system vibration. Trans ASME: J Dyn Syst Meas Control 1990;112(1):76–82.
[9] Onsay T, Akay A. Vibration reduction of a flexible arm by time optimal open-loop control. J Sound Vib 1991;147(2):283–300.
[10] Meckl PH, Seering WP. Experimental evaluation of shaped inputs to reduce vibration of a cartesian robot. Trans ASME: J Dyn Syst Meas Control 1990;112(6):159–65.
[11] Meckl PH, Seering WP. Reducing residual vibration in systems with time-varying resonances. Proceedings of IEEE International Conference on Robotics and Automation, Raleigh, 1987. p. 1690–5.
[12] Meckl PH, Seering WP. Controlling velocity-limited systems to reduce residual vibration. Proceedings of IEEE International Conference on Robotics and Automation, Philadelphia, 1988. p. 1428–33.
[13] Singer NC, Seering WP. Using a causal shaping techniques to reduce robot vibrations. Proceedings of IEEE International Conference on Robotics and Automation, Philadelphia, 1988. p. 1434–9.
[14] Tokhi MO, Azad AKM. Control of flexible manipulator systems. Proc IMechE-I: J Syst Control Eng 1996;210(2):113–30.
[15] Tokhi MO, Poerwanto H. Control of vibration of flexible manipulators using filtered command inputs. Proceedings of International Congress on Sound and Vibration, St. Petersburg, 1996. p. 1019–26.
[16] Tzes A, Yurkovich S. Adaptive pre-compensator for flexible link manipulator control. Proceedings of IEEE International Conference on Decision and Control, Tampa, 1989. p. 2083–8.
[17] Pao LY. Strategies for shaping commands in the control of flexible structures. Proceedings of Japan–USA–Vietnam Workshop on Research and Education in Systems, Computation and Control Engineering, Vietnam, 2000. p. 309–18.
[18] Murphy BR, Watanabe I. Digital shaping filters for reducing machine vibration. IEEE Trans Robot Autom 1992;8(2):285–9.
[19] Singhose WE, Derezinski SJ, Singer NC. Extra-insensitive input shaper for controlling flexible spacecraft. J Guid Control Dyn 1996;19:385–91.
[20] Pao LY, Lau MA. Expected residual vibration of traditional and hybrid input shaping designs. J Guid Control Dyn 1999;22:162–5.
[21] Aoustin Y, Chevallereau C, Glumineau A, Moog CH. Experimental results for the end-effector control of a single flexible robotic arm. IEEE Trans Control Syst Technol 1994;2(4):371–81.
[22] Tokhi MO, Mohamed Z, Shaheed MH. Dynamic characterisation of a flexible manipulator system. Robotica 2001;19(5):571–80.
[23] Azad AKM. Analysis and design of control mechanism for flexible manipulator systems, PhD Thesis. UK: Department of Automatic Control and Systems Engineering, The University of Sheffield, 1995.
[24] Meddins B. Introduction to digital signal processing. Oxford: Newnes; 2000.